Decomposition of amorphous $Zr_{41}Ti_{14}Cu_{12.5}Ni_{10}Be_{22.5}$ alloy: As investigated by small angle neutron scattering

Jun-Ming Liu[a)]
National Laboratory of Solid State Microstructures, Nanjing University, and Center for Advanced Studies in Science and Technology of Microstructures, Nanjing 210093, People's Republic of China, and Hahn-Meitner-Institut Berlin, Bereich NM, 14109 Berlin, Germany

(Received 16 September 1996; accepted for publication 7 February 1997)

In situ small angle neutron scattering has been applied to investigate in details the structural relaxation of amorphous $Zr_{41}Ti_{14}Cu_{12.5}Ni_{10}Be_{22.5}$ alloy between 620 and 673 K and its effect on subsequent crystallization at 673 K. We demonstrate that crystallization in the decomposed alloy is significantly suppressed. It is revealed that spinodal decomposition of the alloy generates a second supercooled liquid phase embedded in the similarly disordered matrix. The second phase achieves a volume fraction of about 10% and exhibits a barlike pattern. Anomalous kinetics of the microstructural coarsening is observed. © *1997 American Institute of Physics.* [S0003-6951(97)02415-7]

Bulk amorphous $Zr_{41}Ti_{14}Cu_{12.5}Ni_{10}Be_{22.5}$ prepared by water quenching at a cooling rate higher than 10 K/s has attracted special attention in the last two years due to its high glass forming ability and excellent mechanical and engineering properties.[1–4] This alloy shows a quite wide supercooled liquid range (SLR) of about 60 K before crystallization and then is a good object to study properties of a deeply supercooled liquid. Significant influence of these properties by decomposition in the SLR has been demonstrated.[4–8] A deep understanding of the decomposition mechanism and kinetics would be of crucial importance.

A series of techniques, including transmission electron microscopy (TEM),[5–7] atom-probe field ion microscopy (APFIM),[5,7] second ion mass spectrometry (SIMS),[9,10] and small angle neutron scattering (SANS)[6,8] have been applied to investigate the decomposition and related diffusion in the SLR. The results achieved seem to lead to contradictory arguments from one to another. A clear picture of the decomposition and its effect on subsequent crystallization have still not been achieved, partially due to the fact that it is technologically difficult to probe early stage of the decomposition.

In this letter, we report the *in situ* SANS investigation of the decomposition in the SLR and crystallization in amorphous $Zr_{41}Ti_{14}Cu_{12.5}Ni_{10}Be_{22.5}$. The bulk samples of the amorphous alloy were prepared as reported previously.[7] The supercooled liquid state of this alloy ranges from 620 to 673 K, as determined by using differential scanning calorimetry. The disklike samples of 10 mm in diameter and 1.0 mm in thickness were used. The experiment was performed in the V4 instrument installed in the BER-II reactor at the Hahn–Meitnet–Institut Berlin of Germany.[11] Neutrons with a wavelength of 0.6 nm were used and the moment transfer, q, covers the range of 0.03–2.00 nm^{-1}. The samples were individually placed into the furnace installed in the SANS spectrometer. The sample temperature can be precisely controlled. The detector of 64×64 cells was cycled between the two assigned distances with an acquisition time of 5 min at each position and with a moving time of 3 min in between the two positions. After careful corrections for the background, transmission and efficiency of the detector, the scattering function $S(q,t)$ at different temperatures and times was achieved.

As the amorphous sample is annealed directly at the crystallization point, 673 K, we observe a crystallization process in the alloy. At $t=0$, there is achieved very weak and almost constant $S(q,t)$ over all range of q, due to the Laue and incoherent scattering contributions. No peak pattern of $S(q,t)$ is distinguished. Up to about 30 min, the scattering reaches almost a saturated state. Here note that after about 10 min the scattering function can be fitted quite well with Porod law.[12] Furthermore, the crystallization is quite limited since down to $q<0.2$ nm^{-1} no deviation of the scattering from Porod law is observed. The interspacing of the crystals is at least larger than 80 nm. The TEM observations confirm this point and the volume fraction of the crystals is estimated to be only 1.0%.

As the alloy is annealed in between 620 and 673 K, decomposition of the alloy into two supercooled liquid phases is observed. The time evolution of the scattering at $T=620$ K is shown in Fig. 1(a). We observe rapid growth and peak shifting of $S(q,t)$ just after the annealing begins. This demonstrates that the alloy decomposition develops without any incubation. The decomposition proceeds quite quickly in the early stage and then significantly decelerates with time. For the scattering in low q range, it grows at $q^{3.0}$. This exponent is less than 4.0, normally achieved for the nucleation event with low volume fraction of precipitates. For the scattering in high q range, after about 60 min, $S(q,t)$ can be roughly fitted with Porod law, i.e., there exists a finite Porod constant, $K(t)=\lim_{q\to\infty} q^4\,S(q,t)$. For all samples annealed in the SLR, even after 1200 min of annealing, the scattering within 0.03 $nm^{-1}<q<2.2$ nm^{-1} does not show a contribution from crystalline phase. This fact reveals that the products of decomposition are still supercooled liquids.

As the sample is again heated up to 673 K after long time annealing in the SLR, considerable change of $S(q,t)$ is detected, as shown in Fig. 1(b). Further growth of $S(q,t)$, not only of the scattering peak, and especially of the low q part, is observed. This phenomenon reflects the formation of crystals in the sample, in addition to the decomposition. We measured the signals at a very low q range where the con-

a)Electronic mail: liujm@nju.edu.cn

 0003-6951/97/70(15)/1968/3/$10.00

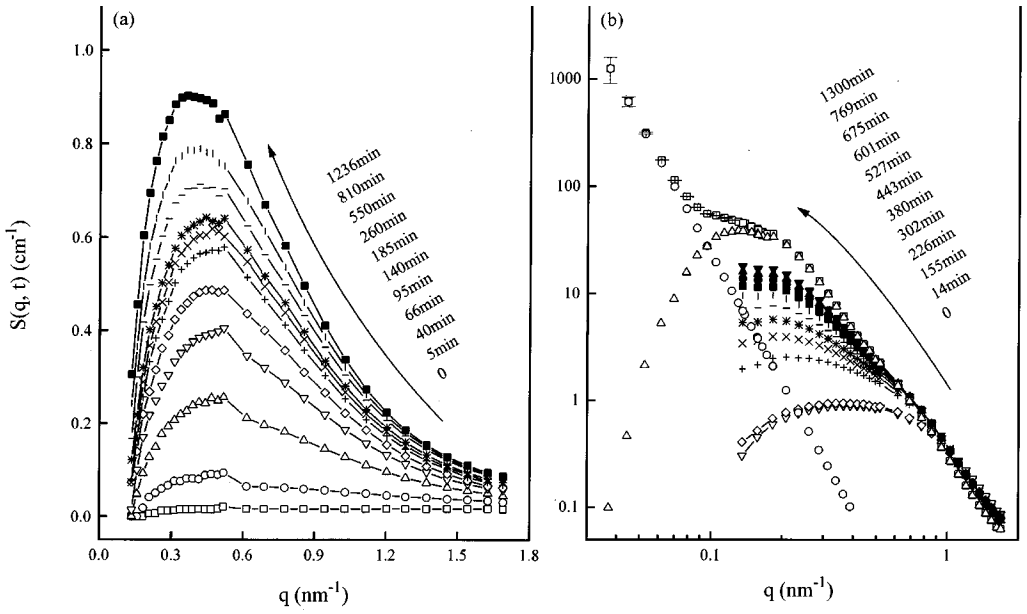

FIG. 1. Time evolution of the scattering spectrum $S(q,t)$ for the amorphous $Zr_{41}Ti_{14}Cu_{12.5}Ni_{10}Be_{22.5}$ samples annealed at 620 K for indicated times (a) and subsequently at 673 K for indicated times (b). The solid arrows indicate time flow. In (b), the open square spots represent the scattering at 1300 min, the open circle spots, and up-triangle spots represent $S_C(q)$ and $S_D(q)$ at this time.

tribution due to the decomposition decays to zero. As an example, the open squared dots in Fig. 1(b) represent the detected signals for sample annealed at 673 K for 1300 min. It is clearly shown that the scattering at $q<0.09$ nm^{-1} can be fitted well by Porod law. This part comes from scattering of the crystals. As extending this part by Porod law toward the high q range, as shown by the open circled dots, we get the scattering from the crystals, $S_C(q,t)$. The scattering from the decomposed supercooled liquids, $S_D(q,t)=S(q,t)-S_C(q,t)$, can be obtained, as shown by the open up-triangle spots. By means of this method, the scatterings due to the crystallization and decomposition at different times are successfully separated.

To understand the influence of the decomposition in the SLR on subsequent crystallization at 673 K, we plot against annealing time the Porod constant $K(t)$ of scattering from the crystals formed at 673 K, as presented in Fig. 2. Because $K(T)$ scales the interfacial area of the crystals with matrix,[12] we immediately come to the conclusion that at 673 K crystallization of the fully decomposed alloy in the SLR is significantly prohibited because $K(t)$ of samples II and III is much lower than that of sample I. Furthermore, because the TEM investigations confirmed that the crystals formed in samples of different thermal history show a similar constitution,[7] the ratio in volume fraction of the crystals between two samples may be formulated as $\mathbf{f}_1/\mathbf{f}_2=[K(1,t)/K(2,t)]^{3/2}$, where f is the volume fraction, and numbers 1 and 2 refer to samples I and II. Assuming the volume fraction of crystals in sample I is f_0, we get the volume fraction in samples II and III with respect to f_0 as a function of annealing time at $T=673$ K. Even after annealing for 1200 min, the volume fraction of crystals in samples II and III is only 36% and 4% of that achieved in sample I, respectively. This processing gives more direct evidence to the conclusion that crystallization in the decomposed alloy is significantly suppressed.

Now we return back to the microstructural evolution during the decomposition in the SLR. We define the nth moment $S_D^2(t)$ and its normalized form $q_n(t)$ of $S(q,t)$ as:

$$S_D^n(t)=\int_0^{q_H} q^n S(q,t)dq+\int_{q_H}^{\infty} K(t)q^{n-4}dq, \quad n=0,1,2,$$
$$q_n(t)=S_D^n(t)/S_D^0(t), \quad n=1,2, \tag{1}$$

where q_H is the high q cutoff of the scattering curve. The first-order moment, q_1, scales the characteristic length of the decomposed microstructure. $S_D^2(t)$ is the invariant of the scattering and can be formulated as $S_D^2(t)=2\pi^2\Delta\eta^2\cdot\phi S_D^2(t)=2\pi^2\Delta\eta^2\cdot\phi\cdot(1-\phi)$.[12] Here ϕ represents the volume fraction of the second phase and $\Delta\eta$ for the contrast factor between the second phase and matrix. Furthermore, applying the Guinier approximation,[12] we get the well-known radius of gyration, $R_g(t)$, which scales the average size of the second phase. The evaluated results show that

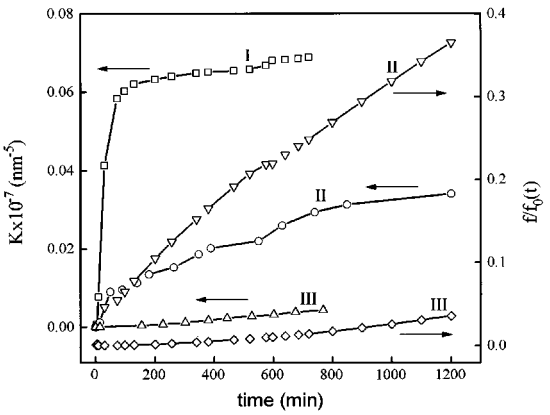

FIG. 2. Porod constant $K(t)$ of the scattering from the crystals formed in the amorphous $Zr_{41}Ti_{14}Cu_{12.5}Ni_{10}Be_{22.5}$ samples as annealed at 673 K after no preannealing (I, open square spots) and preannealed at 643 K for 860 min (II, open circle spots) as well preannealed at 620 K for 1260 min (III, open up-triangle spots), respectively. The open down-triangle spots and open diamond spots represent $f/f_0(t)$, ratio of the volume fraction of the crystals formed in sample II and III to that in sample I.

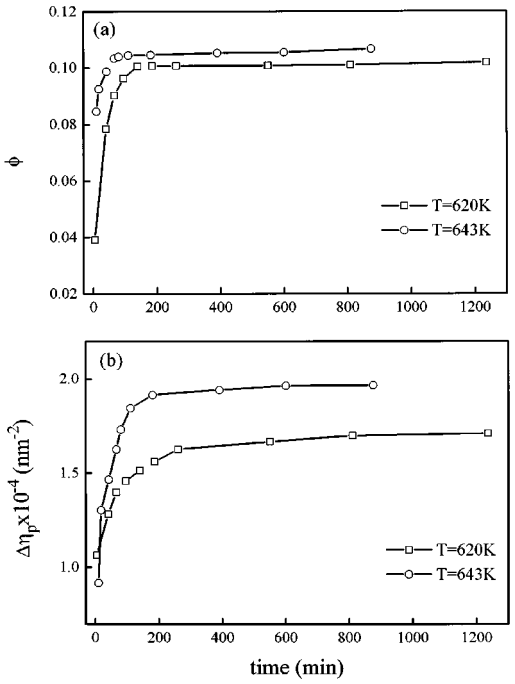

FIG. 3. Time evolution of the volume fraction ϕ of the second supercooled liquid phase (a) and the contrast factor $\Delta\eta_p$ (b) in the amorphous $Zr_{41}Ti_{14}Cu_{12.5}Ni_{10}Be_{22.5}$ samples annealed at 620 and 643 K, respectively.

$2\pi/q_1(t) \gg R_g(t)$. At $T=620$K, toward the late stage, $R_g = 1.8$ nm and $2\pi/q_1 = 8.0$ to 10.0 nm. This fact shows that the second phase exhibits particlelike pattern and occupies quite a low volume fraction. Kinetically, q_1 and R_g depend strongly on annealing temperature. q_1, R_g, and S_D^2 change very rapidly in the early stage ($t<150$ min) and then slow down. We propose a simplified approach of the decomposition. The average density of the second phase particles is $N_p=(q_1/2\pi)^3$ and the average volume per particle is $V_p = 4\pi\theta R_g^3/3$, where θ is a factor for shape correction and equals $(5/3)^{3/2}$ for the spherelike pattern. Therefore, $\phi = N_p V_p$. The evaluated ϕ for the alloy annealed, for example, at 620 K and 643 K, respectively, are given in Fig. 3(a). ϕ increases rapidly in the early stage and then tends to be saturated at about 10%. From the data of ϕ and S_D^2, we obtain $\Delta\eta$. Obviously, the contrast factor between the second phase and homogeneous amorphous structure before decomposition, $\Delta\eta_p$, can be obtained by $\Delta\eta_p=\Delta\eta/(1-\phi)$. The results at $T=620$ and 643 K are presented in Fig. 3(b). It is very interesting that $\Delta\eta_p$ exhibits gradual growth with time, until $t\approx 200$ min. Afterwards it becomes almost saturated. This predicts that the difference between the composition of the second phase and the average composition of the alloy grows gradually. This is direct and ultimate evidence which demonstrates that the decomposition in the SLR follows the spinodal mode. The atom probe spectra of the alloy annealed at $T=620$ K for about 800 min clearly shows that the second phase has a size of 3.8 nm and the interparticle spacing is 8.0 nm, giving $\phi\approx 11\%$. A direct calculation of $\Delta\eta_p$ from the APFIM probed composition profile[7] gives $\Delta\eta_p \approx 1.5\times 10^{-4}$ nm^{-2}, very close to the value obtained from the present SANS data.

Because the sharp interfacial area between the particles and matrix, per unit volume of the sample, is $\Omega_D(t) = \pi\phi(1-\phi)K(t)/S_D^2(t)$, we obtain immediately the shape factor, σ:

$$\sigma(t)=\frac{\Omega_D(t)}{N_p(t)4\pi\frac{5}{3}R_g(t)^2}, \tag{2}$$

which represents the ratio in interfacial area of a particle to a sphere with the same volume. In the early stage, this factor achieves rapid growth. Toward the late stage, we get $\sigma\approx 1.4$–1.5 at $T=620$ K and 1.9–2.0 at 643 K. Both were much larger than 1.0, indicating that the particles deviate from spherical shape. An estimation according to the ellipsoid pattern predicts that the ratio of the two half-axes, a/b, is 2.8 at 620 K and 6.0 at 643 K. This shaped particle looks like a bar rather than an ellipsoid, especially at a higher temperature.

It is well known that the late stage kinetics of a diffusion-controlled decomposition follows the Lifshitz–Slyozov–Wagner (LSW) law with the well approved kinetic exponent, $k=1/3$. For the present alloy, the data of $R_g(t)$ at two temperatures indicate that there exist two time regimes which correspond to the so-called ''early stage'' and ''late stage,'' separately. In both stages, power dependence of time is shown. In the early stage, $k=0.20$ at 620 K and 0.23 at 643 K. These values seem to be very close to the LBM exponent, 0.25.[13] There appears a intermediate regime where the kinetics are significantly slowed down. Toward the late stage, the microstructural coarsening achieves an exponent of 0.06 at 620 K and 0.05 at 643 K. An anomalous and sluggish kinetics of coarsening is shown.

The author is a Ke-Li Fellow, and would like to thank the Alexander von Humboldt-Stiftung of Germany and the Special Program of State Education Commission of China for the financial support of this work. Valuable comments and suggestions from Dr. A. Wiedenmann, Dr. M.-P. Macht, U. Gerold, Dr. N. Wanderka, Q. Wei, and Professor H. Wollenberger are acknowledged.

[1] A. Peker and W. L. Johnson, Appl. Phys. Lett. **63**, 2342 (1993).
[2] W. L. Johnson and A. Peker, in *Science and Technology of Rapid Solidification and Processing*, edited by M. A. Otooni (Kluwer, New York, 1995), p. 25.
[3] Y. J. Kim, R. Busch, W. L. Johnson, A. J. Rulison, and W. K. Rhim, Appl. Phys. Lett. **65**, 2136 (1994).
[4] R. Busch, Y. J. Kim, W. L. Johnson, A. J. Rulison, W. K. Rhim, and D. Isheim, Appl. Phys. Lett. **66**, 3111 (1995).
[5] R. Busch, S. Schneider, A. Peker, and W. L. Johnson, Appl. Phys. Lett. **67**, 1544 (1995).
[6] S. Schneider, P. Thiyagarajan, and W. L. Johnson, Appl. Phys. Lett. **68**, 493 (1996).
[7] M. P. Macht, N. Wanderka, A. Wiedenmann, H. Wollenberger, Q. Wei, H. J. Fecht, and S. G. Klose, Mater. Sci. Forum **225–227**, 65 (1996).
[8] A. Wiedenmann, U. Keiderling, M. P. Macht, and H. Wollenberger, Mater. Sci. Forum **225–227**, 71 (1996).
[9] U. Geyer, S. Schneider, W. L. Johnson, Y. Qiu, T. A. Tombrello, and M. P. Macht, Phys. Rev. Lett. **75**, 2354 (1995).
[10] E. Budke, P. Fielitz, M. P. Macht, V. Naudorf, and G. Frohberg, in *Proceedings of International Conference on Diffusion in Materials*, edited by H. Mehrer (Tarnstec, Winterhur, 1997).
[11] U. Keiderling and A. Wiedenmann, Physica B **213**, 895 (1995).
[12] O. Glatter and O. Kratky, *Small Angle X-ray Scattering* (Academic, London, 1982).
[13] J. S. Langer, M. Bar-on, and H. D. Miller, Phys. Rev. A **11**, 1417 (1975).